Photon-assisted and spin-dependent shot noise in magnetic-field tunable ZnSe/$Zn_{1-x}Mn_xSe$ structures*

Chun-Lei Li(李春雷)[1,†], Yong Guo(郭永)[2,3], Xiao-Ming Wang(王小明)[4], and Yuan Lv(律原)[1]

[1] *Laboratory for Micro-sized Functional Materials, College of Elementary Education, Capital Normal University, Beijing* 100048, *China*
[2] *Department of Physics and State Key Laboratory of Low-Dimensional Quantum Physics, Tsinghua University, Beijing* 100084, *China*
[3] *Collaborative Innovation Center of Quantum Matter, Beijing, China*
[4] *The High School Affiliated to China University of Geosciences, Beijing* 100083, *China*

(Received 29 September 2016; revised manuscript received 22 November 2016; published online 20 December 2016)

We have investigated the photon-assisted shot noise properties in the magnetic field tunable heterostructures. Transport properties of the model structure are strongly dependent on the oscillatory field and the magnetic field. In this structure, electrons can absorb or emit one or multi-photons to reach the quasi-bound state. As a result, the transmission properties are affected considerably by photon-assisted tunneling and these features cause the nontrivial variations in the shot noise and Fano factor. It is found that the shot noise becomes spin-dependent and can be modulated not only by the magnetic field, but also by the oscillatory field. Both the spin-up and spin-down components of the shot noise can be greatly suppressed by the magnetic field, and can also be drastically enhanced by the harmonically driven field. Furthermore, with increasing external magnetic field, it is important to note that the enhanced intensity is decreased, even suppressed. These results suggest another method to suppress the shot noise via modulating the oscillatory field at a diluted-magnetic-semiconductors/semiconductor structure.

Keywords: shot noise, electronic transport, photon-assisted

PACS: 73.21.Ac, 72.25.Dc, 73.50.Td **DOI:** 10.1088/1674-1056/26/2/027301

1. Introduction

Recently photon-assisted tunneling (PAT) in nano-devices has attracted considerable attention due to its potential applications in highly sensitive detectors, high-frequency radiation sources,[1,2] and solid-state quantum bit design.[3,4] PAT usually leads to Fano resonance, which is induced by the interference effect between localized states and the continuum band. Many theoretical approaches have been applied to the calculation of PAT in time-dependent structures.[1,2] Wagner and Zwerger have applied a Fabry–Perot method to study the characteristic scaling parameter of single driven barriers in a driven double-barrier structure.[3] They found an analytic expression for the characteristic scaling parameter of the photonic sidebands that exhibited a strong dependence on the spatial behavior of a driven potential. Using the transfer-matrix technique, Wagner presented tunneling spectrum of a strongly driven double-well structure.[4] In his work, transport properties and quasienergy spectrum have been found to obey completely different scaling laws in the very same structure; Perez del Valle *et al.* researched the field-assisted tunneling in double-barrier with an oscillatory field and gave clear evidence that some drastic changes in the transmissivity occur either when the coupling to the field increases, or the frequency decreases;[5] Nie *et al.* investigated spin-dependent electron transmission through a quantum well[6] and a double-barrier[7] structure. In both cases, a multiplet structure in the transmission spectrum appeared and split into two sets due to the multiphoton process. Tang *et al.* used a Green's function approach to investigate PAT through three quantum dots with spin–orbit coupling.[8] Using the Keldysh nonequilibrium Green's function method, Yuan *et al.* theoretically studied the terahertz PAT in a quantum dot.[9] Some of their ideas for PAT are very much inspired by the terahertz PAT experiment.[10] Their results showed that, to observe the interesting photon-induced excited state resonance in InAs QD, the Coulomb interaction should be larger than the THz photon frequency.

The Mn-based diluted-magnetic-semiconductor (DMS) are prospective candidates for the materials that combine semiconductor behaviors with robust magnetism in application to spintronics devices. II–VI semiconductor low-dimensional structures based on DMS provided us an additional way to optimize the transport properties by using the external electric and magnetic field. The exploration of DMS has been developed since the pioneering work of Gaj *et al.*[11] and Douglas *et al.*[12] After that many creative theoretical and experimental works have been conducted to exploit spin-dependent phenomena. Egues[13] investigated electronic spin filtering in a magnetic-field tunable ZnSe/$Zn_{1-x}Mn_xSe$ heterostructure and found strong spin-filtering effect. Guo *et*

*Project supported by the National Natural Science Foundation of China (Grant No. 11574173), the National Basic Research Program of China (Grant No. 2011CB606405), and the General Program of Science and Technology Development Project of Beijing Municipal Education Commission of China (Grant No. KM201410028021).

†Corresponding author. E-mail: licl@cnu.edu.cn

© 2017 Chinese Physical Society and IOP Publishing Ltd

al.[14–18] have demonstrated several effects in such DMS systems, such as, spin-dependent suppression and enhancement, the electric effect, spin splitting effect. Zhu *et al.*[19] investigated the size dependence of spin-polarized transport through ZnSe/$Zn_{1-x}Mn_xSe$ multi-layer structure and found that the polarization of current density can be reversed in a certain range of magnetic field. While most of the research in this field focus on the time-averaged quantities, relatively less to study the time-dependent properties, such as shot-noise. Shot noise, a non-equilibrium current fluctuation due to the quantization of the charge, is useful to obtain information on a system which is not available through conductance measurements.[20–22] Shot noise is the zero frequency limit of noise power when the bias voltage is sufficiently larger than the thermal energy. For an uncorrelated Poissonian process, the classical shot noise is given by the Schottky formula.[23] In the presence of spin-orbit coupling, the spin degeneracy is lifted so that the spin-up and spin-down electrons present very different transmission. Mishchenko studied shot noise in a system of diffusive ferromagnetic-paramagnetic-ferromagnetic spin valve.[24] Egues *et al.*[25,26] investigated shot noise for spin-polarized currents and entangled electron pairs with spin–orbit coupling in a four-probe geometry and found that shot noise exhibits Rashba-induced oscillations with continuous bunching and antibunching.

Motivated by these investigation, in this paper, we study photon-assisted shot noise in a time-dependent DMS/semiconductor heterostructure (ZnSe/$Zn_{1-x}Mn_xSe$) in the presence of both electric and magnetic fields. The results indicate that the shot noise can be significantly modulated by the oscillatory potential as well as the electric and magnetic fields.

2. Theoretical method

We consider an oscillatory field and magnetic-field tunable three-barrier (for spin-up electron) or three-well (for spin-down electron) structure, shown in Fig. 1, consisting of alternating layers of ZnSe and $Zn_{1-x}Mn_xSe$ (DMS layer). In this system, things become complicated in the DMS layers, due to the giant Zeeman effect caused by the interaction between the conduction electrons and the 3d electrons of the localized magnetic moments of the Mn ions via the sp–d exchange interaction. Within the molecular-field approximation and for a magnetic field along z axis (defined along the growth direction), the giant Zeeman term can be described as $V_{\sigma_z} = -(N_0\alpha)\sigma_z x_{\rm eff}\langle S_z\rangle$. Here σ_z is the electron spin components ($\pm 1/2$ or $\uparrow,\downarrow$) along the magnetic-field direction, $N_0\alpha$ is the electronic sp–d exchange constants in the DMS layer, $x_{\rm eff} = x(1-x)^{12}$ is the effective Mn concentration, and x is real Mn concentration. $\langle S_z\rangle = (5/2)B_{5/2}(5\mu_{\rm B}B/k_{\rm B}T_{\rm eff})$ is the thermal averages of z-th component of Mn^{2+} spin ($B_{5/2}$ is modified 5/2 Brillouin function), $T_{\rm eff} = T + T_0$ is the effective temperature depicting the Mn–Mn interaction phenomenologically, T is the real one and T_0 has been fixed to 1.7 K for a Mn concentration $x = 0.05$.[27] Besides, when we studied the effect of an applied bias FL along the z axis, we needed to add an electric field $-eFz$ to the total Hamiltonian. F is the magnitude of the electric field and $L = L_1 + L_2 + L_3 + L_4 + L_5$ is the total width of the magnetic-field tunable DMS/semiconductor heterostructures. In the absence of any kind of electron scattering, the motion along the z axis is decoupled from the quantized x–y plane that gives Landau levels with energies $E_n = (n+1/2)\hbar\omega_{\rm c}$, where $\omega_{\rm c} = eB/m_{\rm e}^*$ and $n = 0,1,2,\ldots$, $m_{\rm e}^*$ is a single electron effective-mass. Thus, the motion of the electrons can be reduced to a one-dimensional problem, that can be described by the following time-dependent Hamiltonian:[18]

$$H = \frac{1}{2m_{\rm e}^*}\nabla^2 + U_{\sigma_z}(z,t), \tag{1}$$

$$U_{\sigma_z}(z,t) = \begin{cases} 0, & (z<0), \\ V_{\sigma_z}(z) - eFz + V_1\cos(\omega t), & (0<z<L), \\ -eFL, & (z>L). \end{cases} \tag{2}$$

Here $V_1\cos(\omega t)$ is an oscillatory potential with the amplitude V_1 and the frequency ω.

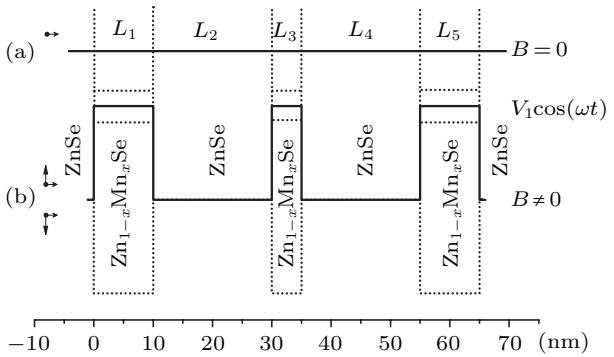


Fig. 1. Schematic plot of the $ZnSe/Zn_{0.95}Mn_{0.05}Se$ multi-layers and conduction band. (a) Zero band offsets potential in the absence of a magnetic field. (b) For nonzero magnetic fields under an oscillatory field $V_1\cos(\omega t)$, for spin-up electrons see three barriers potential, while for spin-down electrons see three wells potential.

Using the Floquet theorem,[28,29] the spin-dependent wave functions in the time-dependent structure can be written as:

$$\Psi_{\sigma_z}(\boldsymbol{r},t) = {\rm e}^{{\rm i}\boldsymbol{k}_{xy}\rho}\begin{cases} \sum_{n=-\infty}^{\infty}({\rm e}^{{\rm i}k_0^{\sigma_z}z - {\rm i}E_0t/\hbar} + r_n^{\sigma_z}{\rm e}^{-{\rm i}k_{en}^{\sigma_z}z - {\rm i}E_nt/\hbar}), & (z<0), \\ \sum_{n,m=-\infty}^{\infty}(a_m^{\sigma_z}{\rm e}^{{\rm i}k_m^{\sigma_z}z} + b_m^{\sigma_z}{\rm e}^{-{\rm i}k_m^{\sigma_z}z}){\rm J}_{n-m}\left(\dfrac{V_1}{\hbar\omega}\right){\rm e}^{-{\rm i}E_nt/\hbar}, & (0<z<L), \\ \sum_{n=-\infty}^{\infty}(t_n^{\sigma_z}{\rm e}^{{\rm i}k_{\rm cn}^{\sigma_z}z - {\rm i}E_nt/\hbar}), & (z>L). \end{cases} \tag{3}$$

Here $\rho = (x, y)$ is the transverse coordinate, k_{xy} is the in-plane wave vector of the transport electrons, the Floquet wave vectors

$$k_0^{\sigma_z} = \sqrt{2m_e^* E_z}/\hbar, \quad k_{en}^{\sigma_z} = \sqrt{2m_e^*(E_z + n\hbar\omega)}/\hbar,$$
$$k_m^{\sigma_z} = \sqrt{2m_e^*(E_z + m\hbar\omega - V_{\sigma_z}(z) + eFz)}/\hbar,$$
$$k_{cn}^{\sigma_z} = \sqrt{2m_e^*(E_z + n\hbar\omega + eFL)}/\hbar,$$

and $J_n(x)$ are the n-th order Bessel functions.

Within the framework of single electron approximation, using the transfer-matrix technique, the total Floquet transmission probability is given as follows:

$$T_n^{\sigma_z} = \sum_{n=0}^{\infty} \frac{k_{cn}^{\sigma_z}}{k_0^{\sigma_z}} |t_n^{\sigma_z}|^2. \tag{4}$$

In this paper, with uniform oscillating potential, both the spatial symmetry and time-reversal symmetry are present in the system, thus no pumped current exists at no temperature bias between the left and right electrodes. The spin-dependent current density through the magnetic-field tunable $ZnSe/Zn_{1-x}Mn_xSe$ heterostructures is given by

$$J^{\sigma_z} = J_0 B \sum_{n=0}^{\infty} \int_0^{+\infty} T_n^{\sigma_z} \{f_l - f_r\} \mathrm{d}E_z, \tag{5}$$

where $f_l = f[E_z + (n+1/2)\hbar\omega_c]$, $f_r = f[E_z + (n+1/2)\hbar\omega_c + eV_a]$, f is the Fermi distribution function, V_a is the bias voltage applied to this structure, and $J_0 = e^2/4\pi^2\hbar^2$.

Using the Floquet scattering matrix,[30] in the low-frequency limit, the spin-dependent shot noise spectral density can be written as follows:

$$S_{\sigma_z} = 2\frac{e^2}{h} \int_0^{\infty} (f_l - f_r)^2 \sum_n T_n^{\sigma_z}(1 - T_n^{\sigma_z}). \tag{6}$$

3. Results and discussion

Throughout this paper we use $m_e^* = 0.16m_e$, $x = 0.05$, $N_0\alpha = 0.26$ eV, $T = 4.2$ K, $T_0 = 1.7$ K, $L_2 = L_4 = 2L_1 = 2L_5 = 4L_3 = 20$ nm, and $E_f = 5$ meV. Figure 2 presents the spin-dependent transmission probability as a function of the incident energy for electrons tunneling through a magnetic-field tunable structures at different photon energies. We take into account different Floquet sidebands both above and below the incident energy, with $n = 0, \pm 1, \ldots, \pm N$. Numerical accuracy is secured for its cutoff $N > V_1/\hbar\omega$.[28] In this case we set $N = 4$.

In Fig. 2, we set $V_1/\hbar\omega = 2$, $B = 5$ T, and $\hbar\omega = 5, 7$, and 10 meV, respectively. For comparison, figures 2(a1) and 2(b1) show the corresponding spin-up and spin-down transmission coefficients for the case without the oscillating field, respectively. It can be easily seen that the transmission coefficients are strongly dependent on the photon energy. This is because a multiple peak structure of the transmission coefficients indicates PAT as a result of the interaction between the electron and the oscillating field. For the spin-up case, as the frequency increases, the expected satellite peaks move towards the direction of high energy and the first resonant split peaks are suppressed. It is due to the fact that a satellite peak appears when the energy difference between the incident energy and quasi-bound state is equal to the energy of one or more photons. As a result, it is possible to control the location of the satellite peaks by adjusting the frequency of the oscillatory field. For the spin-down case, it is important to note that transmission coefficients are enhanced for the lower energy region and they are suppressed for the higher energy region.

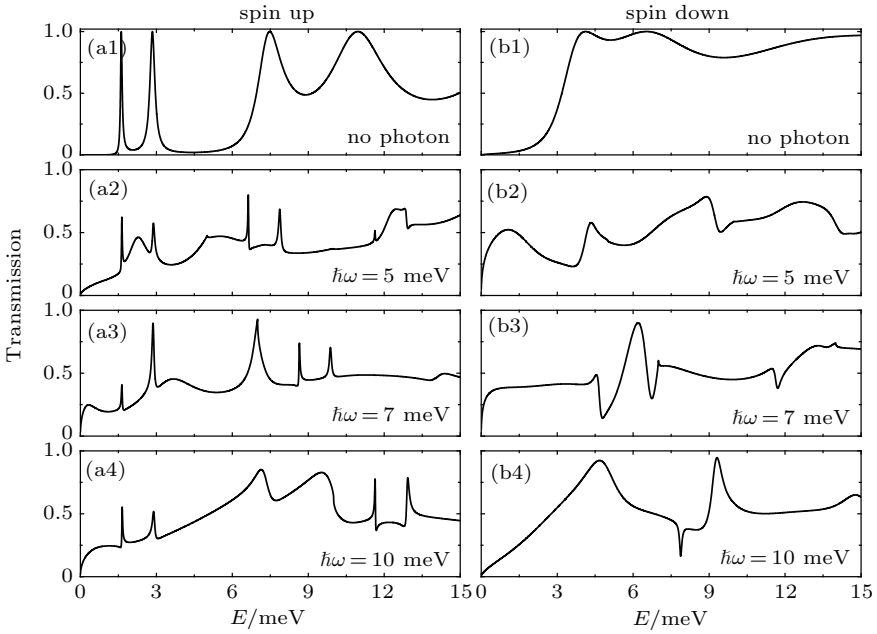


Fig. 2. Spin-dependent transmission for spin-up and spin-down electrons traversing a $ZnSe/Zn_{0.95}Mn_{0.05}Se$ multi-layers heterostructure for different energies of photon. Panels (a1) and (b1) show the transmission without the harmonically driven field. $V_1/\hbar\omega = 2$, $B = 5$ T, and $\hbar\omega = 5, 7$, and 10 meV, respectively.

Figure 3 shows spin-dependent transmission coefficients as a function of the incident energy at different amplitude of the oscillatory field. In Fig. 3, we set $\hbar\omega = 6$ meV, $B = 5$ T, and $V_1 = 0, 6, 12, 18$ meV. From the curves, one can see that the amplitude V_1 greatly changes the transmission coefficients of the electron in the magnetic-field tunable structures. For the spin-up case: at the lower amplitude ($V_1 = 6$ meV), there is a central-resonance-split-peak that is in the same width as the field-free case [Fig. 3(a1)], meanwhile, with some satellite peaks occurring at $E_R + \hbar\omega$ ($E_R = 1.62$, 2.84 meV are the resonant energy levels). With the oscillating field amplitude increasing, the central-resonance-split-peak is suppressed, and the higher-order satellite peaks ($E_R + 2\hbar\omega$) become more obvious. For the spin-down case: with the oscillating field amplitude increasing, the Fano-type resonances broaden and higher-order resonances begin to appear. From what has been discussed above, we may safely draw a conclusion that the energy level for the magnetic-field tunable structures can be determined by the location of the resonances, which can be used to measure the structure parameters of the heterostructures such as thickness and band gaps. It provides a means to adjust the line shape of the asymmetric resonance peaks by external parameters.

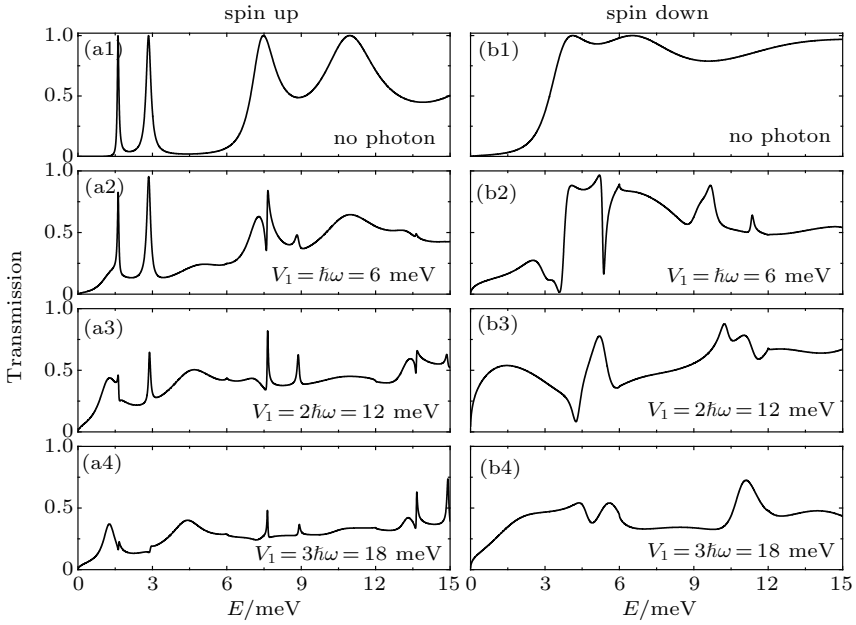


Fig. 3. Spin-dependent transmission for spin-up and spin-down electrons traversing a $ZnSe/Zn_{0.95}Mn_{0.05}Se$ multi-layers heterostructure for different amplitude of the oscillatory field. Panels (a1) and (b1) show the transmission without the harmonically driven field. $\hbar\omega = 6$ meV, $B = 5$ T, and $V_1 = 6, 12$, and 18 meV, respectively.

Figure 4 gives the curves of the photon-assisted spin-dependent shot noise versus the external bias with different external magnetic-field. We set $V_1/\hbar\omega = 2$, $B = 0.5$, 2, 5 T, and $\hbar\omega = 1, 4, 8$ meV. At zero bias, the magnetic-induced potential is a three-barrier for spin-up electrons or a three-well for spin-down ones; as a result, one can see that the shot noise is strongly spin-dependent. It is also shown that both the spin-up and spin-down components of the shot noise are strongly suppressed as the magnetic field increases. This is because that the magnetic field increases the magnitude of the external potential energy via Zeeman interaction and the sp–d exchange between the conduction-band electrons and the three-dimensional electrons of the localized magnetic moments.

Furthermore, the dependence of the shot noise on the photon energy is nontrivial. From Fig. 4, one can see that the shot noise curves show a nonmonotonic dependence with the photon energy. When the oscillatory field is included, the shot noise curves will be complicated by emitting or absorbing photon. At a small magnetic field, both the spin-up and spin-down components of the shot noise are strongly enhanced due to the oscillatory field. However, with increasing the external magnetic field, the degree of the enhancement is weakened. It is also worth mentioning that the shot noise for spin-up component can be suppressed via interplay of the external magnetic field and the photon energy (see Figs. 4(a2) and 4(a3)).

To have a deeper insight into the influence induced by the photon energy, we investigated the Fano factor properties with the different the photon energy. In Fig. 5, we plotted the Fano factor as a function of the applied bias at the different external magnetic fields. The model parameters used here are the same as those used in Fig. 4. From Fig. 5, one can see that the Fano factor for spin-down electrons under the oscillatory field is smaller than that for spin-up ones at all magnetic fields. The reason is that the transmission of the latter case is smaller than the former case, which brings up smaller Fano factor of the shot noise. On the other hand, the spin-up components of

the shot noise and the corresponding Fano factor display oscillatory behavior when the oscillatory field is turned off (see Fig. 4(a3) and Fig. 5(a3)). The reason is that the transmission probability for spin-up electrons demonstrates some sharp optimal resonant peaks at $E = 1.59, 2.84$ meV (see Fig. 2(a1)).

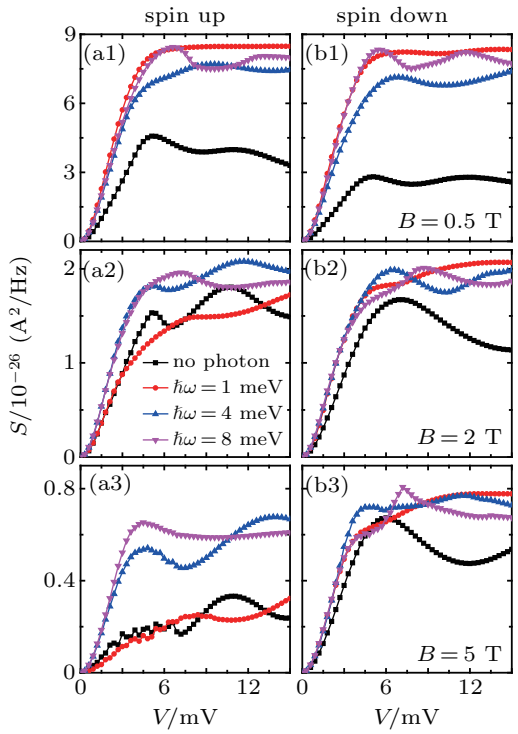


Fig. 4. (color online) Spin-dependent shot noise as a function of the applied bias for ZnSe/$Zn_{0.95}Mn_{0.05}$Se multi-layers heterostructure measured in three different energies of photon and different external magnetic fields. $B = 0.5$, 2, and 5 T, and $\hbar\omega = 1, 4$, and 8 meV, respectively.

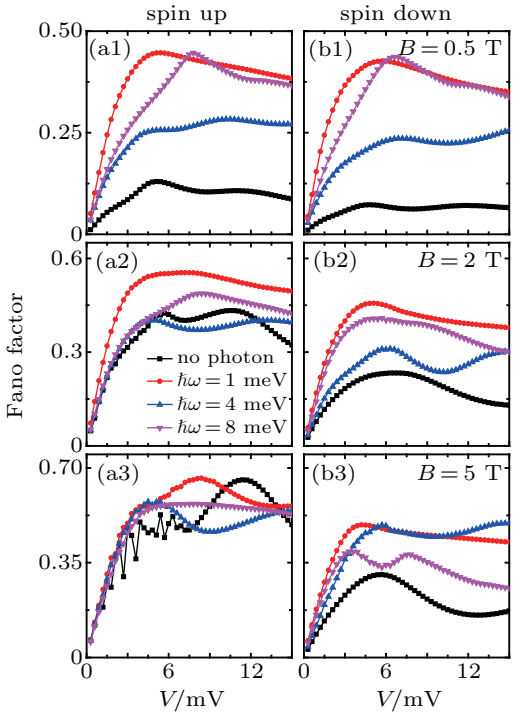


Fig. 5. (color online) Fano factor of the spin-dependent shot noise as a function of the applied bias for ZnSe/$Zn_{0.95}Mn_{0.05}$Se multi-layers heterostructure in three different energies of photon and different external magnetic fields. $B = 0.5$, 2, and 5 T, and $\hbar\omega = 1, 4$, and 8 meV, respectively.

In order to understand the sensitivity to the intensity of the oscillatory field, we plot the spin-dependent shot noise and Fano factor with different intensities in Figs. 6 and 7. The parameters are $\hbar\omega = 6$ meV, $V_1 = 6, 12$, and 18 meV, and $B = 0.5, 2$, and 5 T.

From Fig. 6, one can see that both spin-up and spin-down components of the shot noise, especially for the case of the magnetic fields $B = 0.5$ T and 5 T, are strongly enhanced at all intensities V_1. However, the enhancement trend does not change monotonically with intensity. That is, as the intensity V_1 increases, both of the spin-up and spin-down components of the shot noise increase at first and then decrease at all the magnetic fields. It is important to point out that the spin-up shot noise, under some special conditions (as shown in Fig. 6(a2)), can be suppressed via interplay of the external magnetic field and the intensity V_1.

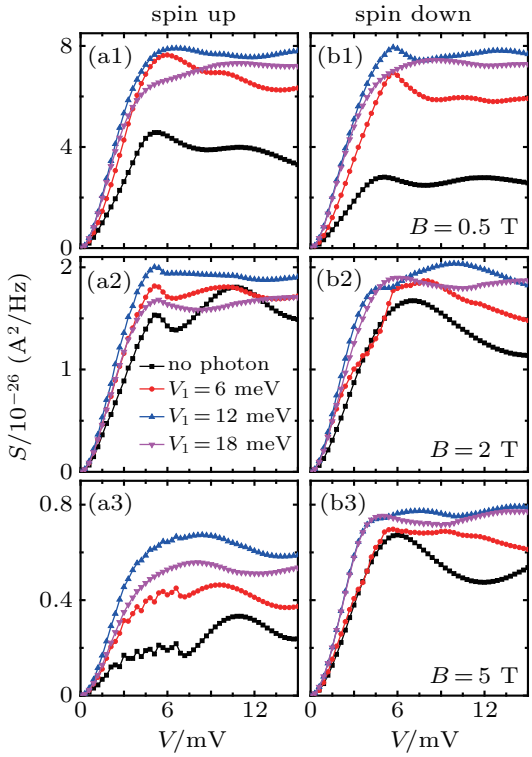


Fig. 6. (color online) Spin-dependent shot noise as a function of the applied bias for ZnSe/$Zn_{0.95}Mn_{0.05}$Se multi-layers heterostructure measured in three different amplitudes of the oscillatory field and different external magnetic fields. $B = 0.5$, 2, and 5 T, $\hbar\omega = 6$ meV, and $V_1 = 6$, 12, and 18 meV, respectively.

In Fig. 7, we present the numerical results of the Fano factor as a function of the applied bias. As the intensity V_1 increases, the spin-down transmission is suppressed (see Figs. 3(b1)–3(b4)), thus the spin-down component of the Fano factor is enhanced. However, compared with the spin-down Fano factor, there is a different behavior for the spin-up case except at the lower magnetic field $B = 0.5$ T. The corresponding spin-up ones show nonmonotonic behavior with the increase of driven intensity V_1. These interesting features may provide useful guidance for devising a tunable spin device.

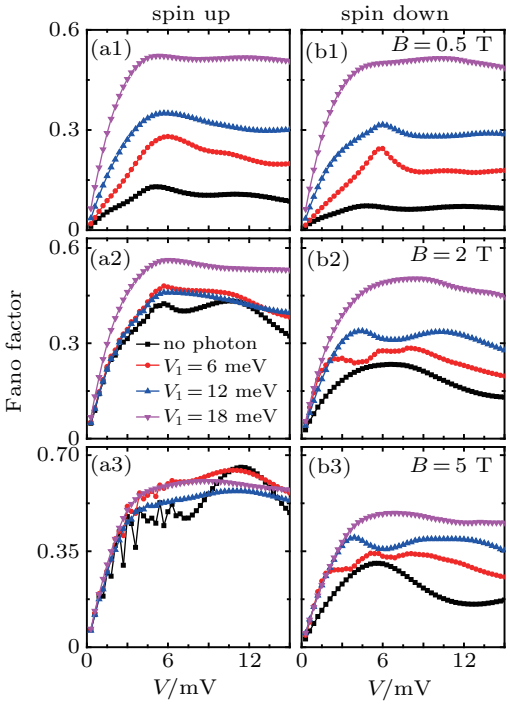


Fig. 7. (color online) Fano factor of the spin-dependent shot noise as a function of the applied bias for $ZnSe/Zn_{0.95}Mn_{0.05}Se$ multi-layers heterostructure in three different amplitudes of the oscillatory field and different external magnetic fields. $B = 0.5$, 2, and 5 T, $\hbar\omega = 6$ meV, and $V_1 = 6$, 12, and 18 meV, respectively.

4. Conclusion

We have investigated the photoassisted shot noise properties associated with spin-dependent tunneling in a DMS/semiconductor structure by using the Floquet theorem and the effective-mass approximation theory. The interplay of the multi-layer structure and the photon-assisted transmission processes plays an important role in the transport properties of the model structure. Electrons can absorb or emit one or multiple photons to reach the new path introduced by photon-assisted resonant path. As a result, the transmission properties are strongly dependent on the oscillatory field. These features cause the nontrivial variations in the shot noise and Fano factor. At moderate oscillatory field strength and frequency, suppression of the shot noise can be found. Our results suggest another method to suppress the shot noise via measuring the photon-assisted shot noise at a DMS/semiconductor structure.

References

[1] Brandes T 1996 *Europhys. Lett.* **33** 629
[2] Wagner M 1994 *Phys. Rev. B* **49** 16544
[3] Wagner M and Zwerger W 1997 *Phys. Rev. B* **55** R10217
[4] Wagner M 1998 *Phys. Rev. B* **57** 11899
[5] Pérez del Valle C, Lefebvre R and Atabek O 1999 *Phys. Rev. A* **59** 3701
[6] Zhang C X, Nie Y H, and Liang J Q 2006 *Phys. Rev. B* **73** 085307
[7] Ye C Z, Zhang C X, Nie Y H and Liang J Q 2007 *Phys. Rev. B* **76** 035345
[8] Tang H Z, An X T, Wang A K and Liu J J 2014 *J. Appl. Phys.* **116** 063708
[9] Yuan R Y, Zhu G B, Zhao X, Guo Y, Yan H, Sun Q and Ji A C 2014 *Phys. Rev. B* **89** 195301
[10] Shibata K, Umeno A, Cha K M and Hirakawa K 2012 *Phys. Rev. Lett.* **109** 077401
[11] Gaj J A, Ginter J and Galazka R R 1978 *Phys. Status Solid B* **89** 655
[12] Douglas K, Nakashima S and Scott J F 1984 *Phys. Rev. B* **29** 5602
[13] Egues J Carlos 1998 *Phys. Rev. Lett.* **80** 4578
[14] Guo Y, Gu B L, Wang H and Kawazoe Y 2001 *Phys. Rev. B* **63** 214415
[15] Guo Y, Lu J Q, Gu B L and Kawazoe Y 2001 *Phys. Rev. B* **64** 155312
[16] Guo Y, Chen X Y, Zhai F, Gu B L and Kawazoe Y 2002 *Appl. Phys. Lett.* **80** 4591
[17] Guo Y, Shang C E and Chen X Y 2005 *Phys. Rev. B* **72** 045356
[18] Li C L, Yuan R Y and Guo Y 2016 *J. Appl. Phys.* **119** 014306
[19] Zhu Z G and Su G 2004 *Phys. Rev. B* **70** 193310
[20] Blanter Ya M and Büttiker M 2000 *Phys. Rep.* **336** 1
[21] Zhu R and Guo Y 2007 *Appl. Phys. Lett.* **90** 232104
[22] Guo Y, Han L, Zhu R and Xu W 2008 *Eur. Phys. J. B* **62** 45
[23] Liu K, Xia K and Bauer G E W 2012 *Phys. Rev. B* **86** 020408
[24] Mishchenko E G 2003 *Phys. Rev. B* **68** 100409(R)
[25] Egues J Carlos, Burkard Guido and Loss Daniel 2002 *Phys. Rev. Lett.* **89** 176401
[26] Egues J Carlos, Burkard Guido, Saraga D S, Schliemann John and Loss Daniel 2005 *Phys. Rev. B* **72** 235326
[27] Yu W Y, Twardowski A, Fu L P, Petrou A and Jonker B T 1995 *Phys. Rev. B* **51** 9722
[28] Li W and Reichl L E 1999 *Phys. Rev. B* **60** 15732
[29] Li C L and Xu Y 2010 *Chin. Phys. B* **19** 057202
[30] Moskalets M and Büttiker M 2004 *Phys. Rev. B* **70** 245305